Finite Element Analysis of Inter Spar Ribs of Composite Wing of Light Transport Aircraft against Brazier Load

Polagangu James*, D. Murali Krishna, Gaddikeri Kotresh and Byji Varughese

Advanced Composites Division, National Aerospace Laboratories, Bangalore-560017, INDIA
E-mail: *james@nal.res.in

ABSTRACT

Inter spar ribs of wing of a transport aircraft is subjected to various types of loads. One of the loads that poses stability problem to the interspar ribs of a wing is brazier load, which arises due to flexure of the wing. This paper describes about the finite element analysis of inter spar ribs of a wing at local level against brazier load. This study has been taken place while converting metal wing in to composite wing. The objective of this study is to reduce the weight penalty to the maximum possible extent by removing material wherever feasible. This paper is limited to discuss about the linear buckling analysis of ribs against brazier load. The buckling factor of ribs under consideration are reported in terms of square root times the eigenvalue obtained from finite element analysis, which represent the nonlinear effect of bending moment on brazier load. This study has helped to reconfigure/redesign the interspar ribs of wing. This has led to substantial weight saving of 2.85 Kg which accounts 15.77% reductions of total mass of inter spar ribs.

Keywords: *Brazier Load, Interspar Ribs, Light Transport Aircraft, Composite Wing, Crimp around Cut Out, Weight Penalty.*

1. INTRODUCTION

Brazier load on an aircraft is not a new term to introduce. The detailed concept of this load and its effects on thin cylindrical shells and thin sections were widely discussed by Brazier,[1] however it has been explained in brief in the following section-5 for ready reference. It is also interpreted and applied in the field of aircraft long ago. The detailed derivation can be obtained from any of academic books on airplane structural design.[2] The importance of the Brazier effect is not simply its existence as a failure mode, which is generally acknowledged to be unlikely to occur. Significance of Brazier effect lies in its contribution to other potential failure modes such as local buckling and material failure as well as its effect on dynamic behaviour due to the non-linearity of the bending response. The analytical solutions of Brazier effect in multi-bay aerofoil sections are given by Luca S Cecchini and Paul M Weaver.[3]

Aggressive weight targets and shortened development time scales in the civil aircraft industry naturally calls for an integration of advanced computer aided optimization methods into overall component design process. Finite element based topology, sizing, and shape optimization tools are typically used as part of a two phase design process.[4] In the present study of design of inter spar ribs, the aid of finite element analysis has been taken in to account. The present investigation is to understand the Brazier effect alone on interspar ribs of a composite wing of light transport aircraft. There are many models and methods of removing material from the civil aircraft components in order to achieve weight target. Previous study on shape topology size topology, shape optimization and mass reduction of aircraft component carried out by other industry[4, 5] and research organizations adopted different methods of removing material from inter spar ribs of metal wing. Much theoretical and experimental work

was carried out earlier on stability of flat plate under compression and shear with reinforced holes in the plates.[6] The buckling strength of square plates increased with reinforcement around hole when subjected to compression, but the buckling stress was insensitive to change in reinforcement shape. In all cases the buckling stress was considerably higher than that for unpierced plates. The shape of reinforcement has a lager influence on buckling stress of square plates with different shape of reinforcement around hole when subjected to shear.

The present study is focused on the size optimization of crimping around cut out and mass reduction of inter spar ribs of composite wing of light transport aircraft. The reduction of mass of ribs resulted from removing vertical gussets from the web of ribs by providing required shape and size of crimping around cut out in the web of rib. The crimping around cut out provided sufficient lateral stability to the ribs against the compressive force that comes upon ribs associated with the Brazier effect. Finite element analysis (MSC/ NASTRAN) is used as a means of study whilst carrying out mass removal procedure, the input from analysis has been taken for reconfigure/redesign of ribs. The present study describes about extraction of bending stresses in the top and bottom skin members, shear flow in the interspar box from finite element model of the wing at global level, determination of Brazier load on ribs of wing at global level, transformation of Brazier load from coarser elements (global model) to finer elements (local model) and its application on ribs. The basic objective of this study is determination of buckling factors from stiffness point of view and determination of failure index from strength point of view using Yamada Sun failure criteria.

2. GEOMETRY OF WING

The plan view of wing is shown in Fig. 1. The airfoil of subject aircraft is GA (W)-2(modified) with constant t/c ratio of 0.15 along the span. The wing is located below the fuselage with a dihedral angle of 4° and an incidence of +2°. The wing has a linear lofted twist of 0^0 at the centre line of the aircraft to –2° at the tip. It is through wing with a span of 14.7 m. The center line chord of wing is of 2.65 m, and tip chord of 0.85 m. The wing area is 25.70 m^2 with an aspect ratio of 8.41. The composite wing of light transport aircraft consists of 23 stations, of which station #1 is situated at the centerline of aircraft and station 23 is situated at tip of wing on both left hand and right hand wings. Left hand and right hand wings together have been divided into three parts. The wing extended from station-6 of left hand wing to the station-6 of right hand wing as a single member called as *inboard* wing. Second and third parts of wing are independent portion of wing extended from station-6 to station-23 of left or right hand wing called as *outboard* wing.

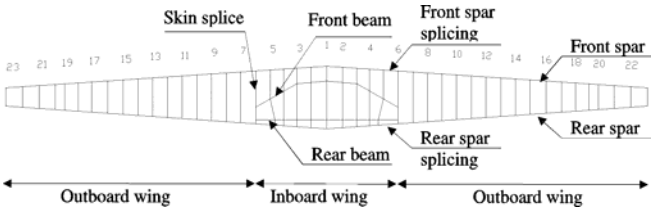

Fig. 1: Geometry of Composite Wing of Light Transport Aircraft

3. CONSTRUCTION OF WING

The metal wing of this particular aircraft was of two spar construction, with 'C' shaped cross section for front spar, rear spars and interspar ribs. Certain modification have been taken place in the cross sections of a few prime load carrying members without compromising the geometry of airfoil of the wing when converted from metal wing in to composite wing. The cross section of front spar, rear spar and interspar ribs are modified in to inverted 'J' section. The wider flange of the front spar, rear spar and interspar ribs except a few are co-cured with the bottom skin and mechanically fastened to the top skin. This co-curing technology eliminates the fasteners which otherwise required to assemble the above parts with the bottom skin. Elimination of fasteners obviously reduces the time required for assembly and the weight of aircraft, besides this it also improves the sealing for the fuel. Top and bottom skins of inboard and outboard portions of wing are joined together at station-6 by means of skin splicing. Front and rear spars of inboard and out board are joined together between station-5 and station-6 by means of spar splicing. It is a well-known fact that much of bending moment resisted by skins and shear force resisted by the spars. Taking the advantage of this concept, moment joint (skin splice) and shear joint (spar splice) are constructed at different locations, instead of constructing at the same location. Construction of skin and spar splicing at different locations avoid the

Table 1: Knockdown Strength Properties of Composite Material G0827-B-1040-HP03-1F Used for Design

S. No	Property (Along fiber direction)	Basic Strength (MPa)	Knock Down Factors			Design Allowable, MPa
			Hole	Bearing	Ageing + temp	
1	Tensile Strength	1300	0.50	0.90	1.00	585
2	Compression Strength	950	0.65	1.00	0.80	494
3	Shear strength	85	0.68	0.80	1.00	46

danger of weak joint at one point. Centerline of the moment joint and shear joint are parted at a distance of 183 mm from station-6 towards station-5.

4. MATERIALS

The composite wing of Light Transport Aircraft is proposed to be fabricated by Vacuum Resin Infusion Technology (VERITy). The carbon epoxy composite material of HS carbon UD fabric G0827-B-1040-HP03-1F is used as reinforcement and RTM 120 and hardener of HY2554 are used for the resin system. The reinforcement is having 97% carbon fibers in the warp direction and 3% glass fibers in the weft. The glass fibers hold carbon fibers together in warp direction. Design allowables under hot wet conditions for laminates at room temperature and hot wet properties of the coupons made by VERITy process have been evaluated as per requirements of FAR. The room temperature and hot wet properties of the coupons made by VERITy process have been evaluated as per requirements. The following are the base line data for unidirectional carbon fiber composites manufactures by VERITy process. The thickness of cured ply is 0.17 mm, the density of cured laminated is 1.5 gm/cc, Modulus for major Poisson's ratio E_L = 130 GPa. Modulus for buckling E_L = 130 GPa if t ≥ 5 mm and E_L = 120 GPa if t ≤ 5 mm, E_T = 8Gpa, G_{LT} = 3Gpa, υ_{LT} = 0.32. The strength properties with knockdown factors are given in Table 1.

5. BRAZIER LOAD

When a wing subjected to bending moment, it tends to produce inward acting loads on the wing inter spar ribs as shown in Fig. 2. Since the inward acting loads are oppositely directed on tension and compression side they tend to compress the ribs. The load which causes the compression of ribs is termed as "**Brazier load**". The inward acting loads which are in the direction of radius of curvature arise from the fact that the normal stress *'σ'* acting on an element of cross section area of wing *dA* and length *ds* along the span of the wing give rise to two forces *σ. dA,* inclined to each other at angle *ds/R* the radial component of these two force is given by Eq. (1), taken reference.[1, 2]

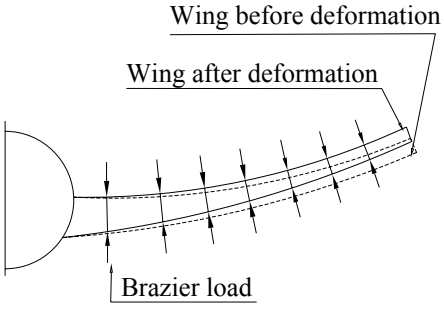

Fig. 2: Brazier Load in Inter Spar Ribs of Wing Structure

$$P = \sigma.dA.\frac{ds}{R} = \frac{\sigma.M.s.A}{EI} = \frac{M^2.s.yA}{EI^2} \quad \ldots (1)$$

The Eq. (1) reduced to Eq. (2) upon substituting appropriate terms from flexural equation,

$$f_{\text{crush}} = \frac{2.N^2}{E.t.h} \quad \ldots (2)$$

6. REASON OF CHOOSING FINITE ELEMENT ANALYSIS

The traditional and theoretical way of calculation of the Brazier load from Eq. (1) required exact values of bending moment, radius of curvature, moment of Inertia of section of the wing. Determination of geometrical parameters like moment of inertia, radius of curvature of the composite wing consisting of various lamination sequences at different sections of the wing, considering the effect of nose box, aft box invites tedious hand calculation. The theoretical calculation of Brazier load distribution along the length of ribs gives only the average numerical value, which does not account the effect of airfoil shape, presence of cut outs in the bottom skin. Finite element analysis of the composite wing at global level for all critical load

cases has already been carried out prior to this study. The reason for choosing finite element analysis for the purpose of reconfiguration and redesign study is to reduce above tedious hand calculation. The crushing stress over a panel length on each rib can be estimated using Eq. (2) along the span of wing, which determines the exact distribution of Brazier load along the length of ribs reflecting the effect of the cut out in the bottom skin. The input required from finite element analysis of the wing for determination Brazier load using Eq. (2) is only the resultant bending stress component acting in the skin members. The resultant bending stress from analysis is more realistic one as the wing model considered the effect of nose box, aft box, an airfoil shape and cut out in bottom skin. The shear flow due to both vertical shear force and torque is always exists simultaneously, they can't be separated independent while designing a shear web panel against shear force. The values of that shear flow around all edges of ribs are also extracted from finite element analysis of wing at global level and applied along with Brazier load on ribs at local level.

7. RECONFIGURATION OF SIZE AND SHAPE OF INTER SPAR RIBS

PT-1 of light transport aircraft consisted of metal wing, in which lightening holes of various shapes and size are made in the web of all interspar ribs as shown in Fig. 3(a), except a few ribs which form the boundary for fuel tank area. These holes in turn reduced the buckling strength of interspar ribs. To increase the stability of ribs sufficient vertical gussets to the web of ribs with Crimp around lightening holes were provided. The same geometrical configuration of ribs has been considered at initial stage of design of composite wing. During the process of design, it has been proposed to introduce changes in the Crimp around lightening holes considering inputs from fabrication point of view. The design and fabrication team decided to remove vertical gussets from the web of ribs as shown in Fig. 3(b) so as to make the fabrication and assemble easy without compromising the stability of ribs against the shear and axial force acting on it. All stringers of top skin are co-cured with top skin. Two stringers of bottom skin bounding cut outs are co-cured with bottom skin and running along the span of the wing. The other stringer of bottom skin are also co-cured but not running through out the span, but extended between adjacent ribs. The cut out for top and bottom stringers to run along the span are also introduced in the web of rib as shown in Fig. 3(b). The stability of ribs lost due to removal of gussets can be set back by providing alternative stiffeners of required size and shape. The question in front of design and analysis team is that what is the size and shape of that stiffener. It was decided to provide the stiffener in the form of crimp around the cut typically in rib-7, rib-11 and rib-12 as shown in Fig. 4(a), Fig. 4(b) and Fig. 4(c) respectively. Irrespective of shape and size of the lightening cut out, the dimensions of the crimp is same. The dimension of crimp is shown in Fig. 5(a) and Fig. 5(b) has been frozen prior to the analysis. In general rib experiences various types of loads. In this study only the Brazier load and shear flow around all edges of rib is considered. Determination of these loads from finite element analysis of the wing at global level is discussed in the following section 7.1 and section 7.2.

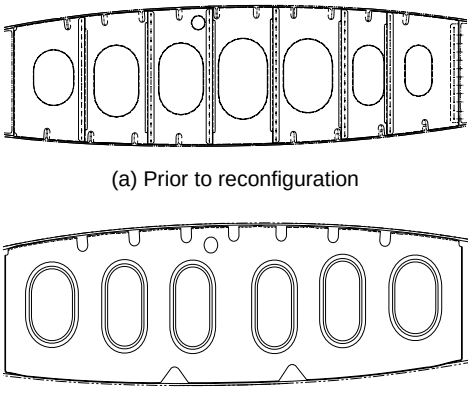

(a) Prior to reconfiguration

(b) After reconfiguration

Fig. 3: Schematic Diagram of Typical Interspar Rib of Composite Wing of Light Transport Aircraft

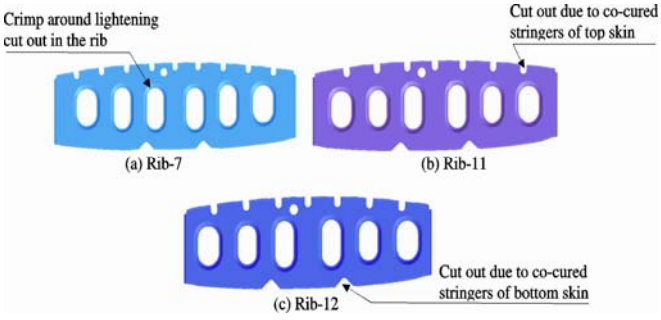

Fig. 4: Three Dimensional Model of Interspar Rib of Composite Wing of Light Transport Aircraft

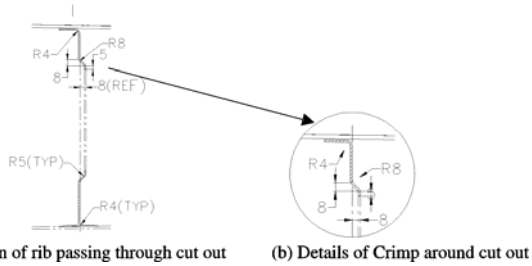

(a) Cross section of rib passing through cut out (b) Details of Crimp around cut out

Fig. 5: Cross Section and Details of Crimp Around the Cut Out in the Ribs of Composite Wing

7.1 Determination of Brazier Load on the Ribs

The first and foremost thing that is required for reconfigure the ribs is the quantity and its distribution of Brazier load acting on each rib under consideration. As discussed in above sections, bending stress resultant component is only input parameter required to determine Brazier load on ribs using Eq. (2). The meshing pattern adopted in top and bottom skin of wing at global level is shown in Fig. 6. The linear static finite analysis has been carried out on the wing at global level for 28 critical flight and landing cases. The load case that induces the maximum bending stress in top and bottom skin has been identified (maximum upward bending). The maximum bending stress resultant component, N (=σ. t) is taken in each element extended between front and rear spar as shown in Fig. 6. The value of N has separately been extracted for top and bottom skins. The Brazier load on top edge of rib due to stress in top skin is calculated using Eq. (2), substituting other parameters like equivalent modulus and thickness of composite top skin. The height of rib is physically measured at centroid of each element along length of rib. The same procedure is also adopted for determining the Brazier load on bottom edge of rib due to stress in bottom skin. The detailed calculation performed for arriving at Brazier load due to stress in top skin at rib-7 of outboard wing is given in Table 2. It is noticed from element-1 to element-20 in Table 2, the variation of Brazier load along the length of rib is captured by taking the input value of resultant bending stress and variation of rib height along the chord. Brazier load calculated on each element along the chord then converted into equivalent load per unit length along the chord as shown in Col-[7]. This unit load again converted in to equivalent point load by multiplying the element width of finer mesh (5 mm) along the chord of local model as given in Col-[8].

7.2 Determination of Shear Flow around All Edges of Rib

The secondary load that is considered in this analysis is shear flow around all edges of ribs. The shear stress resultant from finite element analysis of wing at global level has also been extracted along the lines which connect edges of rib with top skin, bottom skin, front spar and rear spar. Shear flow calculation does not require any equation for its distribution on edges of ribs. The value of shear flow acting in on all edged of rib-7 is tabulated in Table 4. The number of element on top face and bottom face are different for this rib as shown in Fig. 7, whereas the number of element on front and rear spar face are equal. Then the shear flow again converted into equivalent point load on each node of finer mesh (5 mm) adopted in local model as explained in the above section.

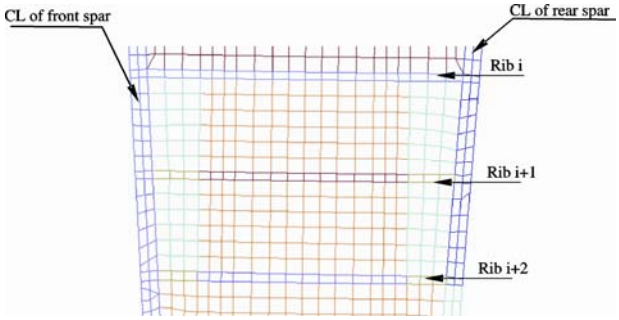

Fig. 6: Schematic Finite Element Model of Top and Bottom Skin of Wing at Global Level

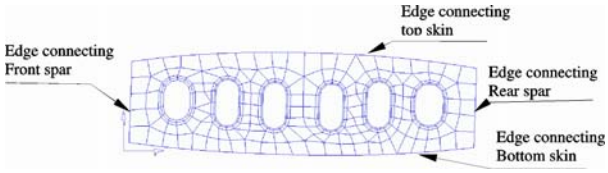

Fig. 7: Finite Element Model of Rib-7 in the Wing at Global Level

8. FINITE ELEMENT MODEL FOR LOCAL ANALYSIS

Given the loading and boundary conditions, the buckling behavior of the structural member varies with the size of element chosen in finite element analysis. Smaller the size of the element more accurate is the mode shape. The element size adopted in the finite element model of the wing at global level was around 50 mm × 50 mm as shown in Fig. 7, where as the element size decided to adopt for the purpose of study the effect of Brazier load

Table 2: Brazier Load on Top Skin Face of Rib-7 of Composite Wing at Global Level

Element No.	*Average Width of Element Along the Chord, mm*	*Resultant Bending Stress Component N/mm*	*Crushing Stress on Rib, MPa*	*Spacing between Adjacent Ribs, mm*	*Brazier Load on Element (Global) , N*	*Force Per Unit Width of Element Along the Chord, N/mm*	*Brazier Load Along Length of Rib (local) , N*
[1]	*[2]*	*[3]*	*[4]*	*[5]*	*[6]*	*[7]*	*[8]*
1	49.00	385.56	6.50E-03	325.5	103.66	2.12	10.58
2	54.50	406.98	6.90E-03	325.5	122.34	2.24	11.22
3	58.00	434.52	7.53E-03	325.5	142.17	2.45	12.26
4	56.50	454.41	7.93E-03	325.5	145.83	2.58	12.91
5	57.50	468.18	8.17E-03	325.5	152.89	2.66	13.29
6	51.00	475.83	8.20E-03	325.5	136.06	2.67	13.34
7	57.50	481.95	8.28E-03	325.5	154.91	2.69	13.47
8	61.50	486.54	8.36E-03	325.5	167.28	2.72	13.60
9	52.50	492.66	8.46E-03	325.5	144.62	2.75	13.77
10	52.00	492.66	8.41E-03	325.5	142.37	2.74	13.69
11	52.00	495.72	8.49E-03	325.5	143.71	2.76	13.82
12	55.00	497.25	8.54E-03	325.5	152.94	2.78	13.90
13	57.50	498.78	8.65E-03	325.5	161.86	2.81	14.07
14	57.50	506.43	8.97E-03	325.5	167.89	2.92	14.60
15	57.00	507.96	9.22E-03	325.5	171.12	3.00	15.01
16	57.50	494.19	8.87E-03	325.5	166.00	2.89	14.43
17	57.50	462.06	7.90E-03	325.5	147.95	2.57	12.87
18	52.50	423.81	6.99E-03	325.5	119.48	2.28	11.38
19	48.00	362.61	5.34E-03	325.5	83.40	1.74	8.69
20	24.00	191.25	1.55E-03	325.5	12.12	0.50	2.52

on ribs is arbitrary chosen around 5 mm × 5 mm as shown in Fig. 8. In fact the same element size could have been adopted in the interspar ribs in the finite element model of the wing at global level. It is due to the fact that the connectivity between 50 mm size element that was adopted for skin and spar members and 5mm size element supposed to be adopt for ribs poses connectivity problem. This required additional efforts and manual interpolation of geometrical parameters using RSPLINE elements between coarser and finer mesh. In order to eliminate this connectivity problem, it gave rise a separate or local analysis of ribs against Brazier load. However, this local analysis of ribs using finer mesh or coarser mesh elements can not capture the poison's effect on ribs due to flexure of wing that would have been induced in the ribs had it been carried out at global level.

Detailed finite element analysis is carried out on the wing at global level as mentioned in above sections. FE modeling techniques used in global wing analysis are used for this analysis. 2D layered shell elements (PCOMP property of NASTRAN) are used to model elastic behavior of composite laminate. A typical mesh used for local analysis of ribs is shown in Fig. 8. Cut out due to stringer of top skin and bottom skin members as shown in Fig. 8 also introduced in the local finite element model. As per actual geometry of rib the top and bottom flange of inverted 'J' sectioned are cut. In this local finite element model the flanges assumed to continue over the stringer cut outs which will facilitate to constrain the node in this area, and also application of Brazier and shear load along the top and bottom edged. The overall buckling behavior of rib does not much depend up on whether the flange area is modeled or not. Because of this flange above the stringer cut out it is expected that the web near that area may be stressed high, whoever this can not be avoided even the flange area of rib is modeled and the Brazier load and shear load applied on gross flange area.

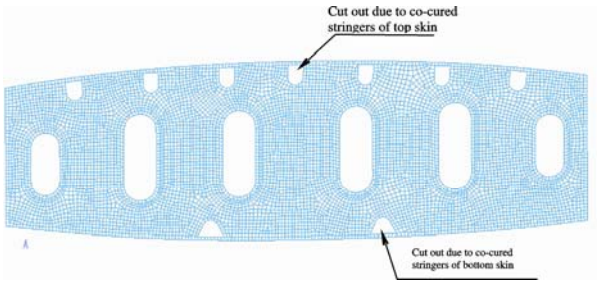

Fig. 8: Finite Element Model of Rib in Local Analysis

9. BOUNDARY CONDITIONS IN FINITE ELEMENT MODEL FOR LOCAL ANALYSIS

The boundary condition applied on rib is shown in Fig. 9(a). The node on edges connecting top skin and bottom skins are restrained against lateral translation only in the direction of span of the wing. The top flange of rib is fastened to the top skin, and bottom flange of the rib co-cured with bottom skin, because of which the two edged of rib deform along with skin members along the span. There is no differential deformation between skin members and ribs. The nodes on edges connecting front and rear spar are restrained against lateral translation in the direction of chord and span of the wing. Similarly these two edges of rib are co-cured with spar members, because of this these two edges of rib deform along with web of spars. There is no differential deformation between spar members and ribs. Only the nodes which are located in four corners of rib are constrained against translation in three directions for getting solution through the software. The boundary condition chosen above made possible to apply Brazier load and shear flow distribution around rib edges. It is also felt that the boundary condition chosen in this problem is only one among different type of boundary condition initial thought of.

10. APPLICATION OF BRAZIER AND SHEAR FLOW ON RIB AT LOCAL ANALYSIS

Referring Table 3, the coarser element vise Brazier load distribution on top edge of rib at global level is

Table 3: Shear Flow Distribution around Rib-7 of Composite Wing at Global Level

Element No in Top Skin (FS to RS)	*Shear Flow, N/mm*	*Element No. in Bottom Skin (FS to RS)*	*Shear Flow, N/mm*	*Element No Front Spar (TS to BS)*	*Shear Flow, N/mm*	*Element No Front Spar (TS to BS)*	*Shear Flow, N/mm*
[1]	*[2],*	*[3]*	*[4]*	*[5]*	*[6]*	*[7]*	*[8]*
1	–530	1	178	1	–337	1	488
2	–447	2	178	2	–324	2	623
3	–374	3	35	3	–307	3	591
4	–306	4	21	4	–316	4	592
5	–297	5	67	5	–348	5	456
6	–230	6	104				
7	–242	7	108				
8	–169	8	139				
9	–128	9	166				
10	–65	10	–737				
11	–57	11	–309				
12	6	12	–109				
13	22	13	–413				
14	92	14	–668				
15	202	15	–108				
16	347	16	–134				
17	209	17	–167				
18	304	18	–264				
19	507	19	–296				
20	927	20	–282				
		21	–400				
		22	–124				
		23	–124				

given in col.-6. Then it has been converted in to equivalent point load on top edges of rib with finer mesh element at local level as given in Col-8. First step, measured the distance of 49 mm given in Col-2, from front spar towards rear spar in finer mesh model, counted the number of nodes covered within 49 mm, then applied 10.58 N point loads on these nodes. Second step, measured the distance 103.50 mm (cumulative distance of first coarser element width of 49 mm and second coarser element width of 54.50 mm) from front spar towards rear spar in finer mesh model, counted the number of nodes on which the load has not yet been applied in the first step. Then applied point load of 11.22 N on these nodes. The step wise procedure continued till the end of the all nodes in finer mesh model. It is ensured that all point loads applied on top and bottom edges of rib are normal to the edge at each node as shown in Fig. 9(b). The same procedure is adopted while applying Brazier load as point load on nodes on bottom edge. The shear flow distribution given in Table 3 is also applied on all faces of rib as explained above. While applying the shear flow as point load it is ensured that the direction of load is in line with the edge of rib as shown in Fig. 9(c).

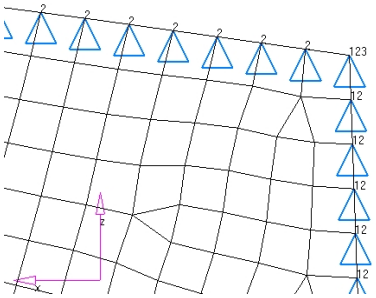

(a) Boundary condition

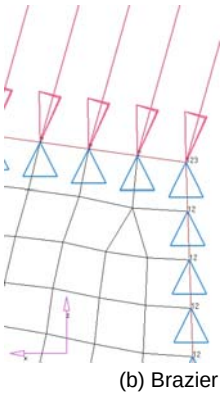

(b) Brazier load

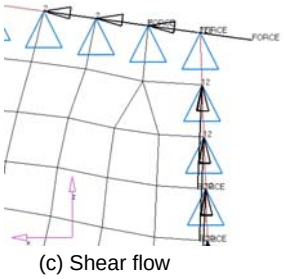

(c) Shear flow

Fig. 9: Boundary Condition and Loading on Finite Element Model of Ribs at Local Analysis

11. VALIDATION OF INPUT FROM FINITE ELEMENT ANALYSIS

To validate the present study on removal of mass from ribs considering the effect of Brazier and shear flow on ribs of composite wing, a supportive study on similar structure is undertaken. For this purpose a regular rectangular box measuring 4000 mm length, 270 mm height and 1200 mm width with ribs placed at regular interval of 400 mm along the span as shown in Fig. 10 has been considered. The thickness of all members is of 3 mm. The top and bottom flange of the box structure represents the top and bottom skins of wing respectively. The two web members of box represent the front and rear spars of wing respectively. The box has been modeled like a cantilever beam subjected to concentrated load at free end as shown in Fig. 10. All the components of the box modeled with mesh size of 50 mm × 50 mm shell element uniformly, for example the meshing pattern adopted for ribs is shown in Fig. 11. A linear static analysis (MSC NASTRAN® v7.0) and geometrical nonlinear static analysis (ABACUS® v6.7.0) had been carried out on auxiliary box. The total stress component along the depth of a typical rib-5 from 3rd column of elements to 6th column of elements as shown in Fig. 11 are extracted and presented in Table 2. The

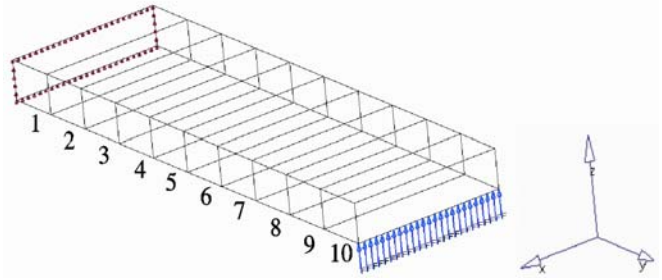

Fig. 10: Schematic Diagram of Auxiliary Rectangular Box Used for Finite Element Analysis for Validation of the Study

Fig. 11: Mesh Pattern Adopted in Inter Spar Rib of Rectangular Box

Table 4: Stress Along the Depth of Rib-5 Obtained from Linear and Geometrical Nonlinear Static Analysis of Auxiliary Box Structure

Element Row	*Stress from Linear Analysis Along the Depth on Z_1*				*Stress from Linear Analysis Along the Depth on Z_2*				*Theoretical Stress*
	Element Column-3	*Element Column-4*	*Element Column-5*	*Element Column-6*	*Element Column-3*	*Element Column-4*	*Element Column-5*	*Element Column-6*	*Average Along Rib*
a	–1.50E-01	–1.35E-01	–1.23E-01	–8.36E-02	1.56E-01	1.46E-01	1.40E-01	1.45E-01	9.96E-04
b	–7.09E-02	–6.28E-02	–4.82E-02	–2.96E-02	8.01E-02	7.83E-02	8.06E-02	8.34E-02	9.96E-04
c	–1.79E-06	1.10E-07	2.33E-06	6.67E-06	–2.30E-06	–6.58E-07	1.18E-06	4.01E-06	9.96E-04
d	7.09E-02	6.28E-02	4.82E-02	2.96E-02	–8.01E-02	–7.83E-02	–8.06E-02	–8.34E-02	9.96E-04
e	1.50E-01	1.35E-01	1.23E-01	8.36E-02	–1.56E-01	–1.46E-01	–1.40E-01	–1.45E-01	9.96E-04
	Stress from Geometrical Nonlinear Analysis Along the Depth on Z_1				*Stress from Geometrical Nonlinear Analysis Along the Depth on Z_2*				
a	–1.48E-01	–1.34E-01	–1.21E-01	–8.35E-02	1.57E-01	1.35E-01	1.42E-01	1.26E-01	9.96E-04
b	–6.95E-02	–6.18E-02	–4.88E-02	–3.28E-02	7.49E-02	7.41E-02	7.40E-02	7.68E-02	9.96E-04
c	1.86E-03	1.45E-03	9.12E-04	8.34E-05	–3.93E-03	–3.52E-03	–2.86E-03	–1.81E-03	9.96E-04
d	7.34E-02	6.51E-02	5.13E-02	3.42E-02	–8.29E-02	–8.15E-02	–8.04E-02	–8.16E-02	9.96E-04
e	1.52E-01	1.37E-01	1.24E-01	8.72E-02	–1.65E-01	–1.43E-01	–1.50E-01	–1.33E-01	9.96E-04

same stress component has also been estimated at rib-5 from theoretical Brazier load using Eq. (2). Upon comparing theoretical stress value with that of analysis stress, it is found that the analysis stress is more than theoretically estimated stress value as given in Table 4. The large difference and variation in stress from theory and analysis attributed to the poison's effect and other several reasons. It is observed from Table 4 that the stress in all elements along the depth of box is symmetrical for linear static analysis and non symmetry for geometrical nonlinear static analysis. The effect of Brazier load therefore captured from geometrical nonlinear analysis. In addition to the above observation, it is noticed that the ribs are subjected to bending in xz plane as the sense of stresses on two face of rib (Z_1 and Z_2) from both linear and geometrical nonlinear analysis are opposite. Understanding of this bending of ribs may be taken up for futures work.

12. RESULTS AND DISCUSSION

Linear static finite element analysis has been carried out on selected ribs. The effect of crimp and shear flow on buckling strength of ribs are studied independently as given in the following sections.

12.1 Effect of Crimp on Buckling Strength of Ribs

The effect of crimp around the lightening cut out of inter spar ribs on its buckling strength was studied. Inter spar rib-11 and rib-12 is considered for the purpose of this study. The reason for choosing these ribs for study is that the thickness of top and bottom skins at these ribs reduced from higher value to the lower values as the Brazier load depends on the thickness and stress resultant acting in the skin members. The estimated brazier load and shear flow distribution on all edges of ribs are applied. The buckling strength of these ribs is studied into two cases. i) In absence of crimp around lightening cut out and ii). In presence of crimp around lightening cut out. The study revealed that the buckling factor of the inter spar ribs is less than 1.00 when the crimping around the cut out is not provided, therefore it is not safe against the compressive load. When the crimping of size shown in Fig. 5 was provided around the cutouts, then the buckling factor increased drastically from 0.46 to 2.88 for rib-11 and from 0.385 to 2.50 for rib-12 respectively. The differences in buckling factors without and with crimping made it clear that there is no need of vertical gussets in the

presence of crimp. The crimping around the cut out is sufficient to carry compressive load safely. The size and shape of crimp shown in Fig. 5 is provided for all cut outs of inter spar ribs irrespective of shape and size of lightening cutout.

12.2 Effect of Shear Flow Distribution on Buckling Strength of Ribs

In addition to the above study, the buckling behavior of inter spar ribs under the application of shear flow (please note that the shear flow is the sum of shear flow due to vertical shear force and torque as both are present simultaneously) distribution acting in the wing structure at its respective position is studied. The same inter spar Rib-11 and Rib-12 is considered for this study also. This study is made in the presence of the same crimp around the cut out as discussed in the above sections. The results revealed that the buckling factor when the shear flow distribution considered is not changed from that value when shear flow was not considered along with Brazier load. Buckling factor of 2.88 and 2.50 for rib-11 and rib-12 are unchanged. This study made it clear that the shear flow on ribs does not change its buckling strength for the boundary conditions adopted in this study.

13. BUCKLING FACTOR

Buckling analysis is carried out on local fine models of rib-2A, rib-5A extended between front spar and front beam in landing gear area of inboard wing and rib-7 to rib-23 extended between front spar and rear spar of outboard wing applying only Brazier and shear flow estimated in above sections. The critical buckling factor (Buckling strength/Applied load at DUL for maximum up bending case) in the inter spar ribs with crimp around the cut out in the web of each ribs have been calculated and presented in Table 5. The typical first mode of buckling of rib-7 to rib-10 is shown in Fig. 12. The buckling strength of rib-12 is the least among all ribs when crimp around the cut is considered. The same rib is considered to carry out the analysis to find the effect of cut out made for stringer run out in the web of rib as shown in Fig. 8. The results revealed that the buckling factor increased from 2.50 to 3.60 in presence of the cut out made for stringer run out, which attributed to the change of load path and this is not true for all ribs.

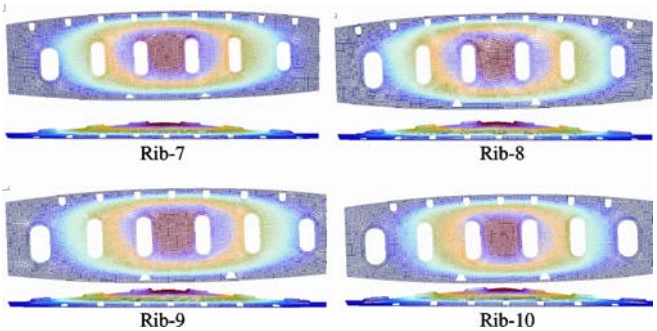

Fig. 12: First Mode of Buckling in Ribs against Brazier Load

Table 5: Buckling Factors and Failure Index Values in the Ribs against Brazier and Shear Loads

No. of the Inter Spar Rib	*Critical Buckling Factor* $\sqrt{\lambda}$	*Failure Index*	*No. of the Inter Spar Rib*	*Critical Buckling Factor* $\sqrt{\lambda}$	*Failure Index*
Rib-2A	2.46	<0.1	Rib-15	2.64	<0.1
Rib-5A	3.39	<0.1	Rib-16	3.11	<0.1
Rib-7	1.97	0.145	Rib-17	3.88	<0.1
Rib-8	2.26	0.112	Rib-18	5.22	<0.1
Rib-9	1.97	<0.1	Rib-19	5.36	<0.1
Rib-10	2.35	0.285	Rib-20	6.96	<0.1
Rib-11	1.70	0.203	Rib-21	>10.00	<0.1
Rib-12	1.58	<0.1	Rib-22	>10.00	<0.1
Rib-13	1.91	<0.1	Rib-23	>10.00	<0.1
Rib-14	2.41	0.12			

Table 6: Weight of Rib of Composite Wing

Name of the Rib	*Weight*	*Name of the Rib*	*Weight*
IS Rib#7	0.990	IS Rib#15	0.392
IS Rib#8	0.917	IS Rib#16	0.392
IS Rib#9	0.846	IS Rib#17	0.321
IS Rib#10	0.825	IS Rib#18	0.286
IS Rib#11	0.549	IS Rib#21	0.210
IS Rib#12	0.502	IS Rib#22	0.178
IS Rib#13	0.477	IS Rib#23	0.286

14. FAILURE INDICES

In order to clear the inter spar ribs from strength point of view, failure indices in most critical ribs have been calculated applying Yamada Sun failure criteria as given in Eq. (3). The stress in each layer is extracted and failure indices are estimated. The most critical ribs from thickness and buckling point of view seen from Table 5 are rib-7, rib-11 and rib-12. The same ribs are considered for the purpose of study of failure indices. The failure indices of these three ribs are found 0.054, 0.053 and 0.021 respectively. In addition to the above study, the effect of cut out made for stringer run out is carried out for rib-12. The failure index for this rib increased from 0.053 to 0.155 when cut out shown in Fig. 5 is considered. The failure index value should be less than 1.00, which is much higher than failure indices obtained from FE analysis. Therefore, the ribs are safe from strength point of view. The failure index values in the ribs are given in Table 5.

$$F.I = \sqrt{\left(\frac{\sigma_{11}}{S_L}\right)^2 + \left(\frac{\sigma_{12}}{S_{LT}}\right)^2} \leq 1.00 \qquad \ldots (3)$$

15. CONCLUSIONS

The projection of crimping around the cut out has been taken into account for the stability analysis. The present study proved that the provision of crimping around lightening holes in the ribs, and elimination of vertical gussets gave enough stability to the ribs to withstand the compressive force induced on it due to the Brazier load and shear flow due to vertical shear and torque. This study suggested to eliminate the vertical gussets thereby reduced the weight of 2.85 Kg from the composite wing by removing 15.77% from interspar ribs alone. The behaviour of ribs needs to be further understood from linear and geometrical nonlinear analysis shown in above sections.

ACKNOWLEDGEMENTS

Authors of this paper thank Director, National Aerospace Laboratories, for financial and scientific support. We wish to thank our B.E students P. Pameshwaran, S. Prashanth, S Sandeep Kamat, V. Siddaraju for carrying out various tests.

NOMENCLATURE

A = Cross section area of skin member under consideration
dA = Cross section area infinitesimal length of skin member under consideration
ds = Infinitesimal length of the wing along the span direction
E = Young's modulus of skin members
f_{crush} = Crushing stress over a one panel length acting on the inter spar ribs in the direction of radius of curvature
h = Height of the inter spar rib at a given point
I = Second moment of inertia of the wing box
M = Bending moment acting at the section of inter spar rib under consideration
N = Normal stress resultant acting in the skin members under consideration.
P = Crushing load acting on the inter spar ribs, N
R = Radius of curvature of the wing box under consideration
S = Spacing between adjacent inter spar rib under consideration
t = Thickness of skin member
y = Height of inter spar rib at the section under consideration
σ = Normal stress acting in the laminate of skin member along axis of bending
σ_{11} = Normal stress in lamina along fiber direction
τ_{12} = Shear stress in lamina
S_L = Allowable stress in lamina
S_{LT} = Allowable in plane shear stress in lamina

REFERENCES

[1] Brazier, L.G., "The Flexure of Thin Cylindrical Shells and Other 'Thin' Sections," *Late of the Royal Aircraft Establishment. Reports and Memoranda*, No. 1081(M. 49), 1926, pp. 1–30.

[2] Sechier (E.E.) and Dunn (L.G.), "Airplane Structural Analysis and Design", Dover Publications Inc, New York, 1963.

[3] Cecchini, Luca S. and Weaver, Paul M., *"The Brazier Effect in Multi-bay Aerofoil Sections*", Palm Springs, California, AIAA 2004–1522, 45th AIAA/ASME/ ASCE/AHS/ASC Structures, Structural Dynamics & Materials Confer 19–22 April 2004.

[4] Krong, Lars; Tucker, Alastair and Rollema, Gerrit, "Application of Topology Sizing and Shape Optimization Methods to Optimal Design of Aircraft Components," Advanced Numerical Simulations Department, Airbus UK Ltd, Bristol, Altair Engineering Ltd., 2002.

[5] Buchanan, Sid, "Development of a Win box Rib for a Passenger Jet Aircraft using Design Optimization and Constrained to Traditional Design and Manufacture Requirements," Bombardier Aerospace, Belfast, Northern Ireland, Altair Engineering Ltd, 2007.

[6] Bulson, P.S., "*The Stability of Flat Plates*," Published by Chatto & Windus Ltd., 1970.

[7] Krishna, D. Murali; Varughese, Byji; Venkatesh, S.; Asha, Kumari; Banker, Manisha M. and Rao, M. Subba, "Analysis of Composite Wing for SARAS Aircraft", PD AC-0715, Advanced Composites Division, NAL, Bangalore, November 2007.

[8] Gaddikeri Kotresh, Polagangu James, Byji Varughese, M. Subba Rao, *et al.*, "Design of Composite Wing for SARAS Aircraft", PD-AC-0714, Advanced Composites Division, NAL, Bangalore, November, 2007.